Temporal stability of the ventral attention network and cognitive function along the Alzheimer's disease spectrum

Evgeny J. Chumin PhD[1,2,4], Shannon L. Risacher PhD[2,3,4], John D. West MS[3,4], Liana G. Apostolova MD[2,3,4,5], Martin R. Farlow MD[4,5], Brenna C. McDonald PsyD[2,3,4,5], Yu-Chien Wu MD, PhD[3,4], Andrew J. Saykin PsyD[2,3,4,5], Olaf Sporns PhD[1,2,3,4]

1. Department of Psychological and Brain Sciences, Indiana University, Bloomington, IN
2. Indiana University Network Science Institute, Bloomington, IN
3. Department of Radiology and Imaging Sciences, Indiana University School of Medicine (IUSM), Indianapolis, IN
4. Indiana Alzheimer Disease Research Center, IUSM, Indianapolis, IN
5. Department of Neurology, IUSM, Indianapolis, IN

Abstract

Understanding the interrelationships of clinical manifestations of Alzheimer's disease (AD) and functional connectivity (FC) as the disease progresses is necessary for use of FC as a neuroimaging biomarker. Degradation of resting-state networks in AD has been observed when FC is estimated over the entire scan, however, the temporal dynamics of these networks are less studied. We investigated the modular structure of static and time-varying FC along the AD spectrum in a two-sample Discovery/Validation design (n=80 and 81, respectively). Cortical static FC networks were estimated for 4 groups (cognitively normal, subjective cognitive decline, mild cognitive impairment, and AD), at 2 brain parcellation resolutions (200 and 300 regions). Time-varying FC was estimated with a sliding window correlation approach. Modularity quality (across a range of spatial scales) did not differ in either static or time-varying approaches. Group differences in temporal stability within and between multiple resting state networks were observed; however, these differences were not consistent between samples. Correlation analyses identified a relationship between cognitive function and temporal stability of the ventral attention network. This relationship was reproduced in both samples, parcellations, and at two different window lengths. While the ventral attention system has been predominantly studied in task-evoked designs, the relationship between its intrinsic dynamics at-rest and cognitive function along the AD spectrum highlights its relevance regarding clinical manifestation of the disease.

Keywords

Alzheimer's disease, functional connectivity, dynamic connectivity, modularity, networks

Introduction

The pathological progression of Alzheimer's disease (AD) is marked by abnormal aggregation of amyloid and tau proteins, neurodegeneration as measured by volumetric reduction in gray matter on magnetic resonance imaging (MRI), cognitive dysfunction, and alterations in brain networks in resting-state and task-based functional MRI (fMRI) (Dennis and Thompson, 2014). Neuroimaging methods such as high-resolution structural MRI have been shown to be valuable disease predictors prior to onset of any cognitive deficits (Jack and Holtzman, 2013, Jack et al., 2013). Structural MRI has been extensively utilized for AD diagnosis in the clinic, and while fMRI has yet to achieve such utility, its application in research has aimed to stratify disease groups (de Vos et al., 2018) and identify relationships between brain function and measures of cognition, blood-based and cerebrospinal fluid biomarkers (Veitch et al., 2019), and genetic risk factors (Quevenco et al., 2017). Recently, numerous studies have focused on linking changes in behavior and/or clinical status to alterations in patterns of structural and functional brain connectivity (Douw et al., 2019, Stam, 2014), including in AD (Tijms et al., 2013).

Connectivity data obtained from fMRI is most commonly analyzed with seed-based, independent component analysis (ICA) (Córdova-Palomera et al., 2017, Fu et al., 2019), and/or graph theory methods (Contreras et al., 2019, Dennis and Thompson, 2014). Graph theory involves the construction of a matrix representation of connectivity across the whole brain, usually defining contiguous nonoverlapping regions/nodes and quantifying their pairwise relationships as a metric of statistical dependence/association (typically Pearson correlation). This functional connectivity (FC) matrix can be subdivided into coherent functional systems or resting-state networks (RSNs) (Yeo et al., 2011, Power et al., 2011). Graph measures indexing functional integration and segregation can be computed from groupwise or individual FC matrices and statistically compared across clinical groups or related to behavioral/cognitive outcomes of interest. Studies that employ graph theory on FC in AD have shown an overall decline in the internal coherence of RSNs (particularly the default mode network (Dai et al., 2019)), a reduction in separation between RSNs (Contreras et al., 2019), and alterations in various global network properties, such as modularity (Dai et al., 2019, Pereira et al., 2016).

Modularity, also referred to as community structure, is a data-driven approach for clustering nodes of a network into groups of densely interconnected regions, or communities (Sporns and Betzel, 2016). Alterations in community structure have been reported in AD, showing higher values in apolipoprotein E ε4 carriers (Wang et al., 2015), higher FC-structural connectivity coupling in the default mode network in AD (Dai et al., 2019), and loss of segregation between default mode and frontoparietal RSNs (Contreras et al., 2019). Despite methodological differences in the application of modularity among these reports, they suggest a common pattern of specific disturbances of FC in AD during resting-state fMRI.

In recent years it has been noted that, within a scan session, significant temporal fluctuations in functional connectivity occur (Lurie et al., 2020, Hutchison et al., 2013), and these fluctuations contain information that is lost when FC is estimated over the entire scan duration. Time-varying functional connectivity (tvFC), aims to capture those temporal fluctuations through estimation of connectivity across discrete or partially overlapping windows (Abrol et al., 2017, Shakil et al., 2016, Allen et al., 2014). To date, tvFC in AD has relied predominantly on ICA-derived FC matrices, and has shown a reduction in internetwork connectivity in AD (Schumacher et al., 2019) and healthy aging (Tian et al., 2018) over the scan duration. tvFC has also shown promise in disease classification via machine learning (de Vos et al., 2018), and tvFC of the dorsal attention/default mode interaction has been related to cognitive

reserve/function in individuals with amnestic mild cognitive impairment (Franzmeier et al., 2017). Previously, Contreras et al. (2019) reported disruptions in modular organization of static (non-time-varying) FC networks along the AD spectrum, particularly involving the frontoparietal and default mode networks. Here we extend this work by investigating stability and dynamics of tvFC community structure stability and its relation to clinical status and behavior.

Methods

Sample Characteristics:

Data were collected as part of the Indiana Memory and Aging Study (IMAS) and from participants enrolled in the Indiana Alzheimer Disease Research Center (IADRC) at Indiana University School of Medicine, Indianapolis, Indiana. Informed consent was obtained from all participants or their representatives, and all procedures were approved by the Indiana University Institutional Review Board in accordance with the Belmont Report. These data were gathered from 161 participants: 55 cognitively normal (CN; 68.24 ± 8.97 years old), 47 with subjective cognitive decline (SCD; 69.23 ± 10.80 years old), 35 with mild cognitive impairment (MCI; 72.54 ± 7.31 years old), and 24 with Alzheimer's disease (AD; 66.42 ± 11.26 years old). A subset of these data were included as part of a previous publication (Contreras et al., 2019). Prior to any analysis of the data, the dataset was randomly split into equally sized Discovery (n=80) and Validation (n=81) samples. Additionally, the authors responsible for analysis were blinded to diagnostic group status of the participants and instead provided with permuted and neutrally coded group labels. Demographic characteristics and diagnostic group distributions for both samples are presented in Table 1. Demographic differences were assessed with an analysis of variance (ANOVA) or chi-squared test, where appropriate.

Table 1. Sample Demographics.

	Sample	
	Discovery	Validation
Age (years)	69.4 ± 8.9	69.0 ± 10.5
Education (years)	16.3 ± 2.4	16.1 ± 2.7
Sex (M/F)	24/56	30/51
Diagnostic Group (CN/SCD/MCI/AD)	29/19/21/11	26/28/14/13

Data are shown as mean ± standard deviation. There were no significant differences between samples. M: Male; F: Female; CN: Cognitively Normal; SCD: Subjective Cognitive Decline; MCI: Mild Cognitive Impairment; AD: Alzheimer's disease.

Image Acquisition:

All participants were scanned on a Siemens 3T Prisma Scanner with a 64-channel head coil (Siemens, Erlangen, Germany). A high-resolution, T1-weighted, whole-brain magnetization prepared rapid gradient echo (MP-RAGE) volume was first acquired with parameters optimized for the Alzheimer's Disease Neuroimaging Initiative (ADNI; http://adni.loni.usc.edu): 220 sagittal slices, GRAPPA acceleration factor of 2, voxel size 1.1 x 1.1 x 1.2 mm^3, 5 min 12 sec duration. Resting-state functional MRI (rs-fMRI) data were acquired with a gradient-echo echo-planar imaging sequence with a multi-band factor of 3, scantime of 10 min 7 sec, and temporal resolution (TR) of 1.2 sec, resulting in 500 timepoints. Other

relevant parameters were TE=29 ms, flip angle 65°, 2.5 x 2.5 x 2.5 mm^3 voxel size, and 54 interleaved axial slices. During the scan, participants were instructed to remain still with eyes closed and to think of nothing in particular. Prior to rs-fMRI acquisition, two spin-echo echo-planar imaging (12 sec each, TR=1.56 sec, TE=49.8 ms, flip angle 90°) were acquired with reverse phase encoding directions, to be used for creating field maps for geometric distortion correction (see Supplementary Methods).

Image Preprocessing:

Data were processed with a pipeline developed in-house, implemented in Matlab and utilizing the Oxford Centre for Functional MRI of the Brain (FMRIB) Software Library (FSL version 6.0.1) (Jenkinson et al., 2012), Analysis of Functional NeuroImages (AFNI; afni.nimh.nih.gov), and ANTS packages. This pipeline was developed and optimized for the Siemens scanner data acquired at Indiana University School of Medicine, based on and following the evidence and recommendations in Satterthwaite et al. (2013), Parkes et al. (2018), and (Lindquist et al., 2019). A brief overview of preprocessing steps is provided below. For details please refer to the Supplementary Methods.

All processing was carried out in each participant's native space. T1 volumes were denoised (Coupé et al., 2008), bias field corrected (FSL), and skull stripped (ANTS). rs-fMRI data were first distortion corrected (FSL *topup*), motion corrected (*mcflirt*), and normalized to a 4D mean of 1000. Nuisance regressors were removed from the data with use of ICA-AROMA (Pruim et al., 2015), aCompCor (Muschelli et al., 2014), and global signal regression. Data were then demeaned, detrended, and bandpass filtered (0.009-0.08 Hz). Finally, 18 timepoints (~22 sec) were removed from the beginning and end of the scan to remove edge artifacts introduced by bandpass filtering.

Network Analysis:

Figure 1 illustrates a diagram of the workflow from regional time series to modularity outcomes.

Parcellation Preparation and Connectivity Matrix Construction:

For each participant, after preprocessing, the final dataset consisted of 464 timepoints. For network construction the Schaefer et al. (2018) cortical parcellation was chosen at two intermediate scales (200 and 300 regions/nodes). Time series for each node were obtained from the average of all voxel time courses within that node. For static FC, the full time series were cross-correlated to obtain a node-x-node matrix of Pearson correlations (Figure1 A-B). All static FC matrices and their histogram distributions of Pearson correlations, as well as sample distributions of the sum of the absolute values of correlations, were inspected, and any participants with abnormal data (sum of the absolute FC outside of 1.5 standard deviations of the mean of the sample) were excluded from the analyses. The remaining participants' static FC matrices were Fisher z-scored prior to analysis. The tvFC matrices were generated with a sliding window correlation approach (Figure1 A, C). Parameters of interest were a 56-timepoint window size (~67 sec; previously reported as adequate duration for FC estimation (Hutchison et al., 2013, Shirer et al., 2011)), step size of 14 time points (resulting in 75% overlap of adjacent windows), and a taper shape of window size/3 (Zalesky et al., 2014). The impact on findings of choosing longer windows (~111 sec) was also investigated.

Modularity:

Both static and tvFC matrices were analyzed with the Louvain community detection algorithm implemented in Matlab (Rubinov and Sporns, 2010, Blondel et al., 2008), aiming to detect communities by maximizing a global modularity measure (Q-metric; Newman and Girvan (2004)). To capture significant modular organization at multiple spatial scales (Jeub et al., 2018, Fortunato and Hric, 2016), we varied a partition resolution parameter γ (gamma) over a wide range, from 0.1 to 4, in steps of 0.1. Due to the stochastic nature of the algorithm, 1000 independent runs of modularity maximization were performed at each of the γ values. From these 1000 runs, the single community partition with the maximal value of the Q-metric was retained. If multiple equally 'good' partitions were identified, the one with the highest frequency across all the runs was selected (Figure 1 C, E).

In order to maintain interpretability of the partitions obtained from modularity maximization and limit the influence of single node communities, a maximum γ value defining the upper bound of the γ range used in further analysis was determined. For static FC this was chosen as the highest γ at which the average number of single node communities across the sample was less than 1. The same approach was employed in tvFC, where the average was determined over all windows and all participants in the sample. Once the γ range was set, subsequent analyses utilized the full spectrum of partitions and/or metrics across the entire parameter range from 0.1 to the determined upper value.

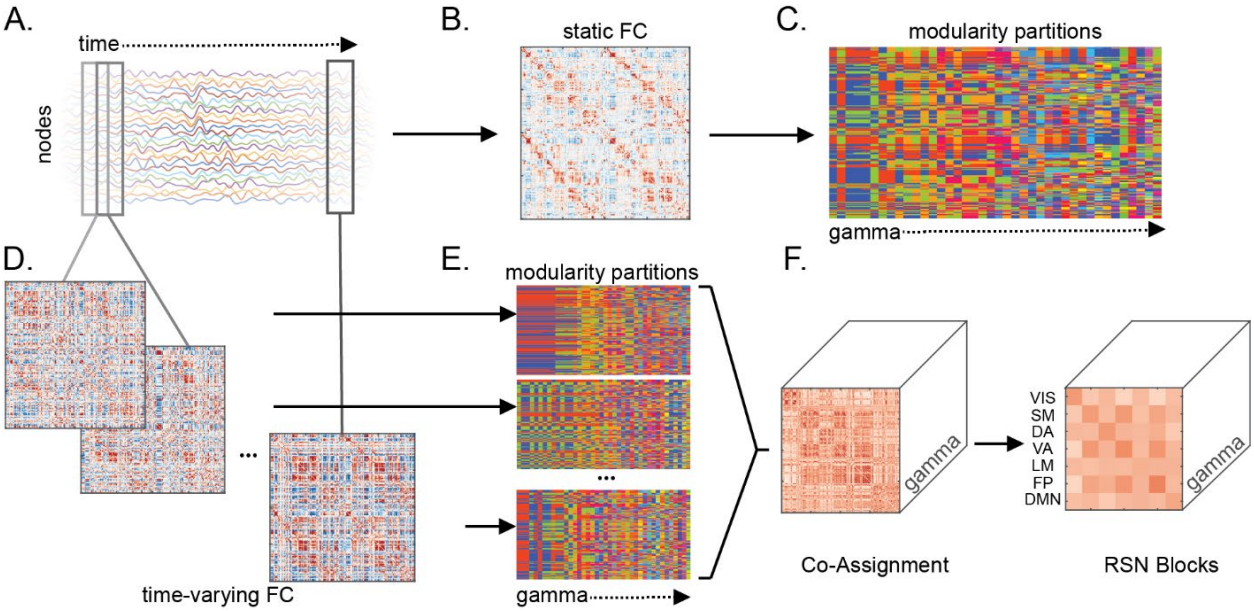

Figure 1. Modularity Analysis Workflow. (Top) Static functional connectivity (FC) workflow. (A) Time series for all nodes were correlated to generate (B) a FC matrix, on which modularity was performed to obtain (C) a set of partitions across γ (gamma) parameter range. (Bottom) Time-varying FC (tvFC) workflow. From time series in A, a sliding window was used to compute (D) tvFC matrices for partially overlapping time frames. (E) A set of modularity partitions was then obtained for each window. (F) For each node pair, Co-Assignment was computed at each resolution over time, which was averaged over canonical resting state network (RSN) blocks. VIS: Visual; SM: Somatomotor; DA: Dorsal Attention; VA: Ventral Attention; LM: Limbic; FP: Frontoparietal; DMN: Default Mode Network

Network Outcomes:

Static FC. The main outcome measures for static FC modularity were the area under the curve (AUC) of the Q-metric and the number of communities over the range of γ values investigated. AUC was chosen as a composite measure of the behavior of a variable of interest across multiple community scales, thus avoiding the need for selection of a specific scale or performing a large number of statistical tests (Fornito et al., 2016).

Time-varying FC. Modularity Q and its AUC across γ were calculated at each window and used to obtain the mean and standard deviation of AUC of the Q-metric over time. Additionally, a Co-Assignment (CA) matrix was computed at each γ over time. In this node-x-node matrix, the values were computed as a ratio of the number of times a node pair was assigned to the same community divided by the total number of partitions (here equal to the number of windows) (Figure 1 F, left). High values indicate that nodes remained associated within the same community across time, while low values indicate that nodes remained separated across time. From these matrices, the mean CA for all nodes within and between bilateral RSNs was computed (Figure 1 F, right). The final tvFC modularity outcome variable of interest was computed as the AUC of CA (referred to as temporal stability) across the investigated γ range.

Neurocognitive Assessments:

All participants underwent a clinical and neuropsychological battery as part of the Uniform Dataset (Weintraub et al., 2018). Data from the following assessments was included: Montreal Cognitive Assessment (MoCA; total score) (Nasreddine et al., 2005), Rey Auditory Verbal Learning Test (RAVLT, immediate and delayed) (Craft et al., 1996), Craft Story (immediate and delayed) (Weintraub et al., 2018), Benson Complex Figure (copy and recall) (Possin et al., 2011), and Digit Span Test (forward and backward) (Weintraub et al., 2018). All scores were adjusted by regressing out age, sex, and education, and subsequently z-scored relative to an independent sample of controls. Finally, the scores were grouped and averaged within three domains: (1) Cognitive Function (MoCA), (2) Memory (RAVLT immediate and delayed, Craft Story immediate and delayed, Benson Complex Figure recall), (3) Attention Processing and Speed (Digit Span forward and backward, Benson Complex Figure copy).

Statistics:

All statistics were carried out in Matlab (MathWorks, version 2019a; Natick, MA). Demographic comparisons among diagnostics groups were carried out with an analysis of variance (ANOVA) or X^2-test where appropriate. Comparisons of network outcomes were performed with a permutation analysis of covariance (ANCOVA), with age, sex, and education as nuisance covariates. Permutations involved randomly permuting group assignments 10,000 times to generate a null distribution of F-values, from which a permutation *p*-value was computed. Where appropriate, post-hoc comparisons were carried out via permutation *t*-tests. Multiple comparisons were subject to a 5% False Discovery Rate (FDR) adjustment when appropriate. Correlations with cognitive domains utilized partial Spearman correlation, adjusting for age, sex, and education.

Supplementary Analyses:

Younger vs. Older AD. AD participants from the Discovery and Validation samples were combined and split into two subgroups based on median age at the time of the scan. Static FC and tvFC outcome

comparisons were carried out at both parcellations to assess possible differences in AD subgroups due to age.

Impact of Splitting the Dataset. After the above-described analyses were completed, we investigated whether the primary results reported here were influenced by the random split of the dataset into the Discovery and Validation samples. Modularity outcome variables for static and time-varying FC (Q-metric, partition number, and temporal stability AUC values) from both samples were pooled together and re-split 500 times, with group comparisons repeated for each split. The proportion of times that a result was consistent between the two samples served as an indicator of robustness.

Results

Sample Characteristics:

Table 2 shows demographic comparisons among diagnostic groups within the Discovery and Validation samples. Overall, the groups were well matched within each sample, with only the Discovery sample showing a significant difference in sex distribution (X^2=8.78, p<0.05). Supplementary Figure 1 shows a more detailed distribution of the demographic variables, which shows that the sex difference in the Discovery sample is driven by greater proportions of females in the cognitively normal (CN) and Alzheimer's disease (AD) groups. Across the three cognitive domains of interest (Cognitive Function, Memory, and Attention and Processing Speed) a significant decline is observed with increasing diagnosis severity, with the exception of Attention and Processing Speed adjusted z-scores, which do not show this pattern to a statistically significant degree in the Validation sample (F=1.89, p=0.14).

Static FC Modularity:

The upper γ value set to limit the appearance of single-node communities was similar for both samples and parcellation scales (Discovery sample: γ=2.7 and 2.8 for the Schaefer 200 and 300 node networks, respectively; Validation sample: 2.8 and 2.3). No significant differences were observed in AUC of modularity Q-metric or number of communities. The curves from which AUC values were computed are shown in Figure 2.

Time-Varying FC Modularity:

Upper γ limits for tvFC were similar to those of static FC networks (Discovery sample: γ=2.6 and 2.6; Validation sample: γ=2.6 and 2.2). No significant differences in mean or standard deviation of the Q metric were observed in the Discovery sample, while the Validation sample showed trend-level differences among groups for both mean (ANCOVA with 10,000 group label permutations, p=0.068) and standard deviation (p=0.07) (Figure 3). Temporal stability (AUC of CA) was compared among diagnostic groups for 28 RSN network blocks (7 within-network and 21 interactions). Several network blocks in both samples and at both parcellation resolutions showed differences at uncorrected significance of p<0.05 (Figure 4), however, none survived FDR corrections when adjusting for the 28 network blocks. Increasing the window size to 93-time points (~111 seconds), produced very similar results (Supplementary Figure 2).

Relationships to Cognitive Function:

Temporal stability for four network blocks significantly correlated (p<0.05 uncorrected) with one of three cognitive domains at both parcellation scales in the Discovery sample: (1) visual-default mode

Table 2. Sample Characteristics

Discovery Sample					
	CN	SCD	MCI	AD	Stats
N	29	19	21	11	
Age (years)	69.9±7.8	68.4±9.3	70.8±7.8	66.6±12.9	n.s.
Education (years)	16.5±2.4	16.5±2.4	16.3±2.5	15.3±2	n.s.
Sex (M/F)	4/25	8/11	10/11	2/9	*p<0.05*
Cognitive Function (z-score)	-0.2±1.3‡§	-0.4±0.9‡§	-2.3±1*^§	-6.3±2*^‡	*p*<0.05E-15
Memory (z-score)	-0.2±0.7‡§	-0.2±0.5‡§	-2.1±0.9*^	-2.7±1.7*^	*p*<0.05E-9
Attention and Processing Speed (z-score)	-0.1±0.9‡	0±0.8‡	-0.8±0.8*^	-1.1±0.9	*p*<0.05
Validation Sample					
N	26	28	14	13	
Age (years)	66.4±9.9	69.8±11.8	75.1±5.8	66.2±10.2	n.s.
Education (years)	16.4±2.3	16.5±2.7	15.4±2.8	15.5±3.2	n.s.
Sex (M/F)	5/21	11/17	8/6	6/7	n.s.
Cognitive Function (z-score)	0.1±1‡§	-0.6±1.2‡§	-2±1.5*^§	-5.5±2.7*^‡	*p*<0.05E-12
Memory (z-score)	-0.1±0.8‡§	-0.3±0.8‡§	-1.5±0.7*^§	-3.1±0.5*^‡	*p*<0.05E-7
Attention and Processing Speed (z-score)	-0.2±0.7	-0.2±0.7	-0.7±0.8	-0.8±1.3	n.s.

Data are shown as mean ± standard deviation. P-values represent significance for a 4-way analysis of variance or X^2-test where appropriate. For distributions of sex see Supplementary Figure 1. CN: Cognitively Normal; SCD: Subjective Cognitive Decline; MCI: Mild Cognitive Impairment; AD: Alzheimer's disease; n.s.: non-significant; M: Male; F: Female; * significantly different from CN; ^ significantly different from SCD; ‡ significantly different from MCI; § significantly different from AD.

interaction block and memory domain (Spearman's rho -0.27, *p*=0.032 and -0.28, *p*=0.027 for 200 and 300 node parcellations, respectively); (2) somatomotor-default mode interaction block and attention/processing speed (Spearman's rho -0.28, *p*=0.025 and -0.29, *p*=0.019); (3) ventral attention network block and the cognitive function domain (Spearman's rho 0.31, *p*=0.011 and 0.32, *p*=0.006); and (4) limbic network block and attention/processing speed (Spearman's rho -0.28, *p*=0.023 and -0.26, *p*=0.039). Those four relationships were subsequently probed in the Validation sample, where only the relationship of temporal stability of the ventral attention network and the cognitive function domain remained significant and survived FDR adjustment (Figure 5, left; *p*=0.003, rho=0.34 and *p*=0.005, rho=0.33, for 200 and 300 node parcellations, respectively). This relationship remained significant with a longer window (Figure 5, right; rho=0.33, *p*=0.005 and rho=0.28, *p*=0.018, for 200 and 300 node parcellations, respectively).

Exploratory Analyses:

Younger vs. Older AD comparisons. The median age of all AD participants used to separate the younger and older AD (yAD and oAD, respectively) was 65.5 years. Neither years of education nor sex differed between the two AD groups. Among modularity outcomes of conventional FC (AUC of modularity Q-metric and number of communities), the Q-metric was significantly lower (*t*-test, *p*<0.05) in oAD (11.74 ± 1.48) than in yAD (12.96 ± 0.99) in the 200 node but not the 300 node parcellation (Supplementary

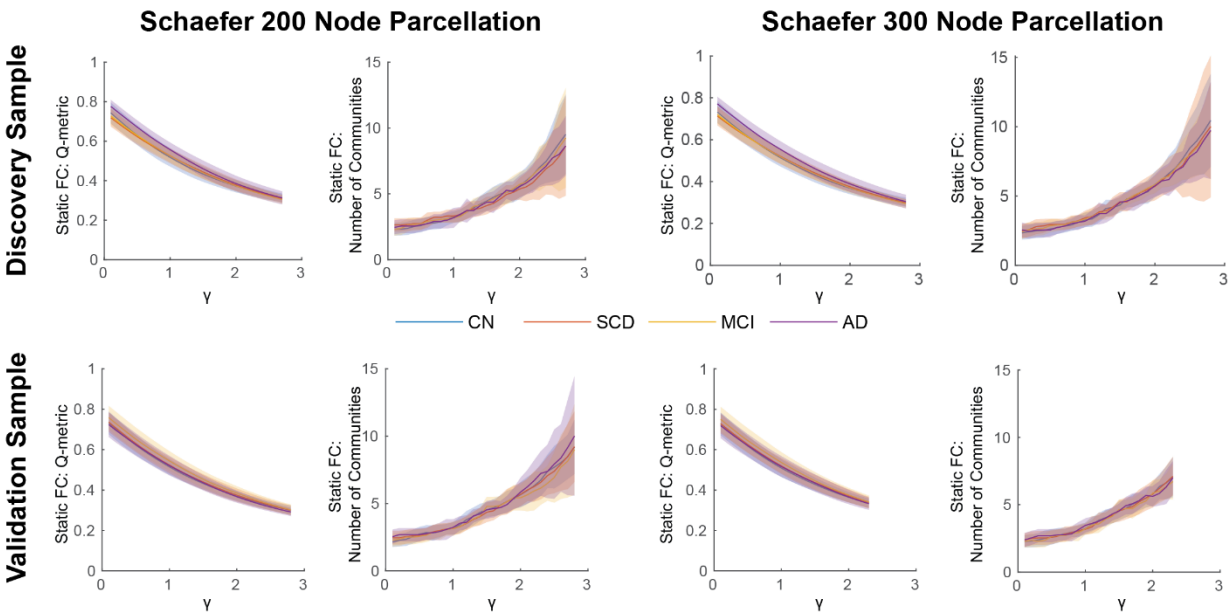

Figure 2. Static Functional Connectivity (FC) modularity outcomes did not differ between diagnostic groups. Modularity Q-metric and number of communities are shown for the 200 node (Left) and 300 node (Right) parcellations from the Discovery (Top) and Validation (Bottom) samples. Data are shown as mean ± standard deviation within group at each of the investigated gamma (γ) resolution values. CN: Cognitively Normal; SCD: Subjective Cognitive Decline; MCI: Mild Cognitive Impairment; AD: Alzheimer's Disease

Figure 3A). No significant differences were found for tvFC in the mean or standard deviation of the Q-metric over time. Temporal stability of community structure significantly differed (*t*-test, FDR-adjusted $p<0.05$) only in the 200 node parcellation for the visual network block ($p=0.0004$), the somatomotor-limbic interaction block ($p=0.0051$), and the ventral attention-limbic interaction block ($p=0.0015$). In all three RSN blocks, yAD had higher temporal stability values (Supplementary Figure 3B-D).

Impact of Splitting the Dataset. Repeated splits of the dataset into two samples produced results in line with those reported above. Supplementary Table 1 shows the reproducibility of findings obtained from the 'original' split of the dataset expressed as a ratio (# of replicated results/500 total splits). Additionally, the consensus between samples (# of times the two samples produced the same result/500) is shown. For temporal stability, in both parcellations the frontoparietal network block had the highest reproducibility of significance (0.026 and 0.076, for the 200 and 300 node parcellations, respectively), however these values were still extremely low. Across both samples and parcellations the fraction of significant outcomes of the frontoparietal network block was 0.018 (9/500 random splits; Supplementary Figure 4).

Discussion

In recent years, functional neuroimaging has been increasingly utilized to study the consequences of AD in vivo, resulting in new insights into location and extent of functional disruptions in the brain. The application of network science has allowed us to analyze fMRI data as a system (network) of individual elements (brain regions) and their interactions (correlation of blood-oxygen-level-dependent signal). In

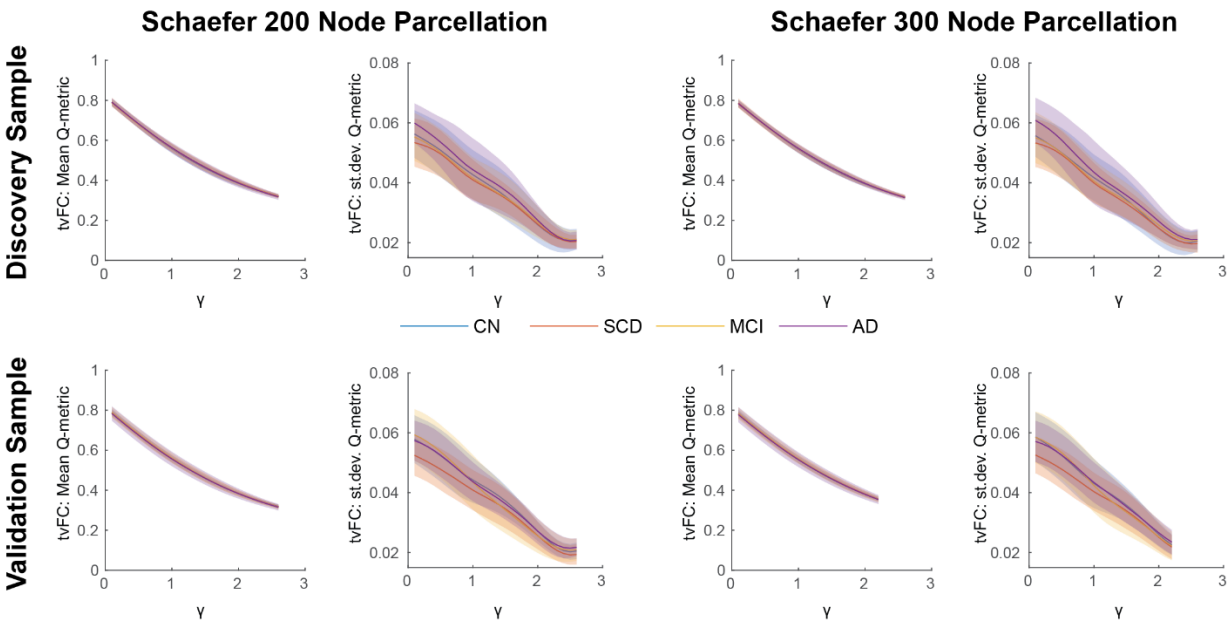

Figure 3. Time-varying Functional Connectivity (tvFC) modularity outcomes did not differ between diagnostic groups. The mean and standard deviation of modularity Q-metric are shown for the 200 node (Left) and 300 node (Right) parcellation from the Discovery (Top) and Validation (Bottom) samples. Data are shown as mean ± standard deviation within group at each of the investigated gamma (γ) resolution values. CN: Cognitively Normal; SCD: Subjective Cognitive Decline; MCI: Mild Cognitive Impairment; AD: Alzheimer's Disease

this study, we focused on the temporal dynamics of brain function in AD by examining the stability of community structure, at rest, in a sample of four groups that spanned the AD severity continuum. In a robust, two-sample (Discovery and Validation) design, we identified a reproducible relationship of temporal stability within the ventral attention network and overall cognitive function. Lower stability, measured as a weakened propensity of VAN regions to associate within the same network community across time, was significantly associated with lower levels of performance. We found no persistent/reproducible differences in commonly reported modularity outcomes (Q-metric, its mean and standard deviation over time, and number of communities).

Prior applications of modularity analyses vary with respect to the algorithm used to cluster the data. The two most often seen approaches utilize either the Louvain algorithm (Blondel et al., 2008, Rubinov and Sporns, 2010, Contreras et al., 2019, Brier et al., 2014, Onoda and Yamaguchi, 2013) or k-means clustering (Ma et al., 2020, Schumacher et al., 2019). When investigating the community structure of static FC networks (computed via average over total scan duration), we did not find any group differences when using the area under the curve (AUC) of Q-metric or number of communities over the γ resolution range. Other studies that utilized the Louvain algorithm have shown a relationship of the Q-metric with age for a predefined community partition (Brier et al., 2014), for a single γ value (Onoda and Yamaguchi, 2013), and for multiscale modularity outcomes (Contreras et al., 2019) over the full γ range. To our knowledge, no studies have utilized AUC in order to assess modularity differences that are consistent over a range of γ values. AUC can be a robust outcome measure for metrics that are

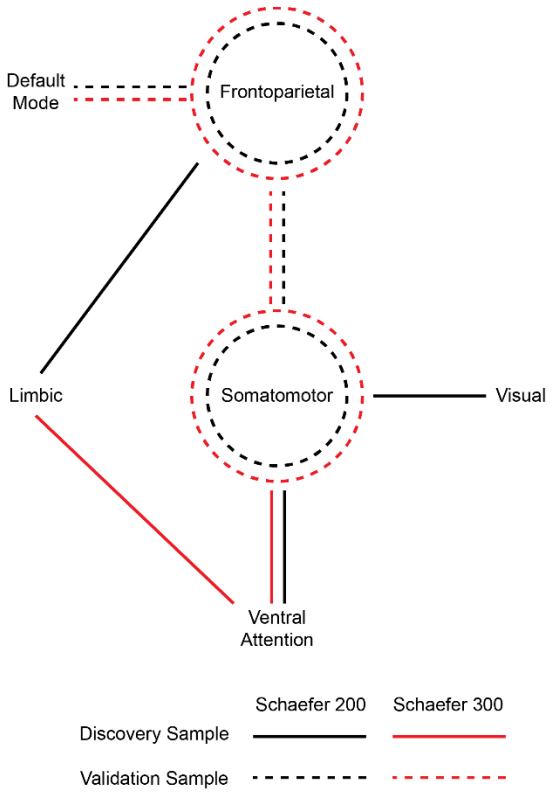

Figure 4. Diagram representation of resting state network differences in temporal stability at uncorrected $p<0.05$. Solid lines indicate differences in the Discovery sample and dashed lines are for the Validation sample. The color of the line indicates parcellation scale of either 200 (black) or 300 (red) nodes.

dependent on free parameters (i.e., the γ resolution parameter in modularity), as it can capture behavior over a range of parameter values and reduce the number of statistical comparisons.

Either during performance of a task or at rest, blood-oxygen-level-dependent signal is always fluctuating, in part due to moment-to-moment changes in neuronal activity. It is now generally accepted that these temporal dynamics are meaningful for our understanding of brain function (Hutchison et al., 2013, Allen et al., 2014). Time-varying FC is often quantified via a sliding window approach, where partially overlapping segments of data are used to study temporal changes in outcomes of interest. In AD, this method has shown that patient groups spend more time in a connectivity state characterized by weak correlations (Fu et al., 2019, Schumacher et al., 2019). These studies utilized a k-means clustering procedure to identify these states and did not directly probe the modular structure of those networks. Here we used the Louvain algorithm to assess variability in modularity (AUC of the Q-metric), similar to the approach utilized in Hilger et al. (2020). We found no difference in average or standard deviation of the Q-metric across diagnostic groups. Visual inspection of the curves in Figure 3 shows the group averages overlapping one another over the full γ range, indicating that the lack of difference is not due to AUC computation.

Hilger et al. (2020) referred to temporal stability as the variance in the modularity Q-metric. Here we used Co-Assignment (CA) (Jeub et al., 2018) as an index of temporal stability, similar to Contreras et al.

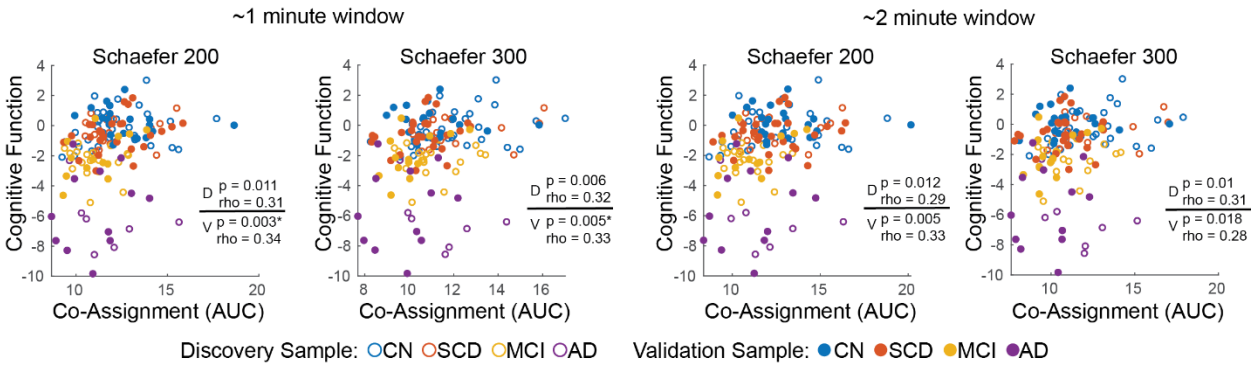

Figure 5. Relationship of cognitive function and temporal stability of the ventral attention resting state network. Individual points represent individual participants from either the Discovery (D, hollow circles) or Validation (V, solid circles) samples, colored by diagnostic group. AUC: area under the curve; CN: Cognitively Normal; SCD: Subjective Cognitive Decline; MCI: Mild Cognitive Impairment; AD: Alzheimer's Disease P-values and Spearman's rho are from age-, sex-, and education-adjusted partial correlations, with asterisks (*) indicating FDR-adjusted significance.

(2019), in which CA was computed from partitions across spatial scales to investigate coherence and coupling of RSNs in static FC. We computed CA over time (across all sliding windows) to investigate stability of community assignments within and between cortical RSNs. For 28 unique cortical RSN blocks (7 within network and 21 interaction blocks), commonly implicated networks emerged when group comparisons were carried out (Figure 3 and Supplementary Figure 2 for longer window size), such as default mode and frontoparietal involving systems (Hohenfeld et al., 2018). However, our findings did not replicate in our two-sample design and none of the differences survived FDR-adjustment for the 28 network blocks.

We assessed whether the random split of the dataset into Discovery and Validations samples influenced our outcomes by performing an additional 500 random splits and repeating all statistical comparisons on the outcome metrics. Results from this analysis demonstrated a high degree of consensus with the original dataset split (Supplementary Table 1 and Supplementary Figure 4), which indicates that the absence of reproducibility of group differences (or lack thereof) in our study is not a chance occurrence. It has been shown that FC differs as a function of age of onset of AD (Pini et al., 2020); therefore, in order to assess whether our findings are influenced by a heterogeneous AD sample we performed a median split on the AD patient group based on age at time of scan and compared older and younger patients. The median age was 65.5 years, which is consistent with generally accepted criteria for classification of early and late onset Alzheimer's disease. Our results showed that younger AD patients had higher Q-metric AUC (static FC) as well as higher temporal stability of visual, somatomotor-limbic, and ventral attention-limbic network interaction blocks. These observed differences did not overlap with any findings among our diagnostic groups, and while they are in themselves intriguing, they must be further addressed in larger samples before any definitive interpretations can be made.

Correlation analysis of RSN temporal stability and neuropsychological domains (cognitive function, memory, and attention processing and speed) showed a single robust and reproducible relationship of cognitive function and the ventral attention network. This relationship was seen across the two window sizes, at both parcellation scales, and in both Discovery and Validation samples (Figure 5). The ventral

attention network is active during orientation to salient targets (Fox et al., 2006, Yeo et al., 2011). It has been shown to activate during a short-term memory task in AD in a manner that did not significantly differ from controls (Kurth et al., 2019), and an ICA-derived ventral attention network was shown to be preserved in AD (Li et al., 2012). The temporoparietal junction, a key node in the ventral attention networks, has been shown to have altered connectivity to the posterior cingulate cortex in AD patients with poor orientation for time performance, relative to AD patients with good performance (Yamashita et al., 2019). Our index of cognitive function was derived from the total Montreal Cognitive Assessment score, which captures several cognitive domains, such as memory, attention, executive function, language, and reasoning, which require attention and orientation to stimuli. Therefore, it is plausible that lower stability of the ventral attention system contributes toward observed deficits in cognitive function.

There are important methodological considerations and limitations to be considered in the interpretation of the presented findings. First, data preprocessing strategies can impact the final FC estimates. The strategy employed here is one that is well suited for dynamic FC analyses and has been shown to produce reliable network estimates (Parkes et al., 2018). Additionally, tvFC and modularity require free parameter choices, such as choice of window size, number of modularity iterations, and resolution parameter range. We aimed to address these issues by choosing a shorter and longer window size, running a high number of iterations (1,000) of modularity, and utilizing area under the curve across a range of the resolution parameters. Finally, splitting the dataset resulted in moderate sample sizes (~80 participants per sample). While larger samples are always preferred in order to conduct sufficiently powered analyses, we believe the validation opportunity provided by the two-sample strategy is more advantageous for identification of robust findings.

In conclusion, we investigated modular structure of static and tvFC in a sample of four groups along the AD continuum. We report a robust relationship between cognitive function and temporal stability of the ventral attention network. Time-varying connectivity investigations of resting-state and task-based fMRI data in conjunction with network science remain promising approaches that may offer unique insight into the neurobiological consequences of AD and could inform clinical interventions as well as biomarker and treatment development.

Declaration of Interest: none.

Author Contributions

Evgeny Chumin: Conceptualization, Methodology, Formal Analysis, Software, Writing-Original Draft. **Shannon Risacher:** Methodology, Resources, Data Curation, Funding Acquisition. **John West:** Resources, Data Curation. **Liana Apostolova:** Funding Acquisition. **Martin Farlow:** Funding Acquisition. **Brenna McDonald:** Writing-Review & Editing, Funding Acquisition. **Yu-Chien Wu:** Writing-Review & Editing, Funding Acquisition. **Andrew Saykin:** Writing-Review & Editing, Supervision, Funding Acquisition. **Olaf Sporns:** Conceptualization, Methodology, Software, Writing-Original Draft, Writing-Review & Editing, Supervision.

Acknowledgements

The authors thank Eileen Tallman, Aaron Vosmeier, Rachael Deardorff, Bradley Glazier, Kala Hall, Lili Kyurkchiyska, Evan Finley, Yolanda Graham-Dotson, Steve Brown, Sujuan Gao, for their contributions to

this study. We also thank the participants in the Indiana Memory and Aging Study (IMAS) and their family members without whom this research would not be possible.

Funding

This work was supported by the National Institute on Aging (R01 AG19771, P30 AG10133, K01 AG049050, R01 AG061788), the National Institute for Complementary and Integrative Health (R01 AT009036-03), the Indiana University Network Science Institute, the Department of Radiology and Imaging Sciences, the Indiana University Health-Indiana University School of Medicine Strategic Research Initiative, and the Indiana Clinical and Translational Sciences Institute (CTSI). Part of this research was also supported in part by Lilly Endowment, Inc., through its support for the Indiana University Pervasive Technology Institute, and in part by the Indiana METACyt Initiative. The Indiana METACyt Initiative at Indiana University was also supported in part by Lilly Endowment, Inc. This material is based upon work supported by the National Science Foundation under grant no. CNS-0521433.

References

ABROL, A., DAMARAJU, E., MILLER, R. L., STEPHEN, J. M., CLAUS, E. D., MAYER, A. R. & CALHOUN, V. D. 2017. Replicability of time-varying connectivity patterns in large resting state fMRI samples. *NeuroImage,* 163**,** 160-176.

ALLEN, E. A., DAMARAJU, E., PLIS, S. M., ERHARDT, E. B., EICHELE, T. & CALHOUN, V. D. 2014. Tracking Whole-Brain Connectivity Dynamics in the Resting State. *Cerebral Cortex,* 24**,** 663-676.

BLONDEL, V. D., GUILLAUME, J.-L., LAMBIOTTE, R. & LEFEBVRE, E. 2008. Fast unfolding of communities in large networks. *Journal of Statistical Mechanics: Theory and Experiment,* 2008**,** P10008.

BRIER, M. R., THOMAS, J. B., FAGAN, A. M., HASSENSTAB, J., HOLTZMAN, D. M., BENZINGER, T. L., MORRIS, J. C. & ANCES, B. M. 2014. Functional connectivity and graph theory in preclinical Alzheimer's disease. *Neurobiology of Aging,* 35**,** 757-768.

CONTRERAS, J. A., AVENA-KOENIGSBERGER, A., RISACHER, S. L., WEST, J. D., TALLMAN, E., MCDONALD, B. C., FARLOW, M. R., APOSTOLOVA, L. G., GOÑI, J., DZEMIDZIC, M., WU, Y.-C., KESSLER, D., JEUB, L., FORTUNATO, S., SAYKIN, A. J. & SPORNS, O. 2019. Resting state network modularity along the prodromal late onset Alzheimer's disease continuum. *NeuroImage: Clinical,* 22**,** 101687.

CÓRDOVA-PALOMERA, A., KAUFMANN, T., PERSSON, K., ALNÆS, D., DOAN, N. T., MOBERGET, T., LUND, M. J., BARCA, M. L., ENGVIG, A., BRÆKHUS, A., ENGEDAL, K., ANDREASSEN, O. A., SELBÆK, G. & WESTLYE, L. T. 2017. Disrupted global metastability and static and dynamic brain connectivity across individuals in the Alzheimer's disease continuum. *Scientific Reports,* 7**,** 40268.

COUPÉ, P., YGER, P., PRIMA, S., HELLIER, P., KERVRANN, C. & BARILLOT, C. 2008. An Optimized Blockwise Nonlocal Means Denoising Filter for 3-D Magnetic Resonance Images. *Medical Imaging, IEEE Transactions on,* 27**,** 425-441.

CRAFT, S., NEWCOMER, J., KANNE, S., DAGOGO-JACK, S., CRYER, P., SHELINE, Y., LUBY, J., DAGOGO-JACK, A. & ALDERSON, A. 1996. Memory improvement following induced hyperinsulinemia in alzheimer's disease. *Neurobiology of Aging,* 17**,** 123-130.

DAI, Z., LIN, Q., LI, T., WANG, X., YUAN, H., YU, X., HE, Y. & WANG, H. 2019. Disrupted structural and functional brain networks in Alzheimer's disease. *Neurobiology of Aging,* 75**,** 71-82.

DE VOS, F., KOINI, M., SCHOUTEN, T. M., SEILER, S., VAN DER GROND, J., LECHNER, A., SCHMIDT, R., DE ROOIJ, M. & ROMBOUTS, S. A. R. B. 2018. A comprehensive analysis of resting state fMRI measures to classify individual patients with Alzheimer's disease. *NeuroImage,* 167**,** 62-72.

DENNIS, E. L. & THOMPSON, P. M. 2014. Functional Brain Connectivity Using fMRI in Aging and Alzheimer's Disease. *Neuropsychology Review,* 24**,** 49-62.

DOUW, L., VAN DELLEN, E., GOUW, A. A., GRIFFA, A., DE HAAN, W., VAN DEN HEUVEL, M., HILLEBRAND, A., VAN MIEGHEM, P., NISSEN, I. A., OTTE, W. M., REIJMER, Y. D., SCHOONHEIM, M. M., SENDEN, M., VAN STRAATEN, E. C. W., TIJMS, B. M., TEWARIE, P. & STAM, C. J. 2019. The road ahead in clinical network neuroscience. *Network Neuroscience,* 3**,** 969-993.

FORNITO, A., ZALESKY, A. & BULLMORE, E. T. 2016. Chapter 11 - Statistical Connectomics. *Fundamentals of Brain Network Analysis.* San Diego: Academic Press.

FORTUNATO, S. & HRIC, D. 2016. Community detection in networks: A user guide. *Physics Reports,* 659**,** 1-44.

FOX, M. D., CORBETTA, M., SNYDER, A. Z., VINCENT, J. L. & RAICHLE, M. E. 2006. Spontaneous neuronal activity distinguishes human dorsal and ventral attention systems. *Proceedings of the National Academy of Sciences,* 103**,** 10046-10051.

FRANZMEIER, N., BUERGER, K., TEIPEL, S., STERN, Y., DICHGANS, M. & EWERS, M. 2017. Cognitive reserve moderates the association between functional network anti-correlations and memory in MCI. *Neurobiology of Aging,* 50**,** 152-162.

FU, Z., CAPRIHAN, A., CHEN, J., DU, Y., ADAIR, J. C., SUI, J., ROSENBERG, G. A. & CALHOUN, V. D. 2019. Altered static and dynamic functional network connectivity in Alzheimer's disease and subcortical ischemic vascular disease: shared and specific brain connectivity abnormalities. *Human Brain Mapping,* 40**,** 3203-3221.

HILGER, K., FUKUSHIMA, M., SPORNS, O. & FIEBACH, C. J. 2020. Temporal stability of functional brain modules associated with human intelligence. *Human Brain Mapping,* 41**,** 362-372.

HOHENFELD, C., WERNER, C. J. & REETZ, K. 2018. Resting-state connectivity in neurodegenerative disorders: Is there potential for an imaging biomarker? *NeuroImage: Clinical,* 18**,** 849-870.

HUTCHISON, R. M., WOMELSDORF, T., ALLEN, E. A., BANDETTINI, P. A., CALHOUN, V. D., CORBETTA, M., DELLA PENNA, S., DUYN, J. H., GLOVER, G. H., GONZALEZ-CASTILLO, J., HANDWERKER, D. A., KEILHOLZ, S., KIVINIEMI, V., LEOPOLD, D. A., DE PASQUALE, F., SPORNS, O., WALTER, M. & CHANG, C. 2013. Dynamic functional connectivity: Promise, issues, and interpretations. *NeuroImage,* 80**,** 360-378.

JACK, CLIFFORD R. & HOLTZMAN, DAVID M. 2013. Biomarker Modeling of Alzheimer's Disease. *Neuron,* 80**,** 1347-1358.

JACK, C. R., JR., KNOPMAN, D. S., JAGUST, W. J., PETERSEN, R. C., WEINER, M. W., AISEN, P. S., SHAW, L. M., VEMURI, P., WISTE, H. J., WEIGAND, S. D., LESNICK, T. G., PANKRATZ, V. S., DONOHUE, M. C. & TROJANOWSKI, J. Q. 2013. Tracking pathophysiological processes in Alzheimer's disease: an updated hypothetical model of dynamic biomarkers. *The Lancet Neurology,* 12**,** 207-216.

JENKINSON, M., BECKMANN, C. F., BEHRENS, T. E. J., WOOLRICH, M. W. & SMITH, S. M. 2012. FSL. *NeuroImage,* 62**,** 782-790.

JEUB, L. G. S., SPORNS, O. & FORTUNATO, S. 2018. Multiresolution Consensus Clustering in Networks. *Scientific Reports,* 8**,** 3259.

KURTH, S., BAHRI, M. A., COLLETTE, F., PHILLIPS, C., MAJERUS, S., BASTIN, C. & SALMON, E. 2019. Alzheimer's disease patients activate attention networks in a short-term memory task. *NeuroImage: Clinical,* 23**,** 101892.

LI, R., WU, X., FLEISHER, A. S., REIMAN, E. M., CHEN, K. & YAO, L. 2012. Attention-related networks in Alzheimer's disease: A resting functional MRI study. *Human Brain Mapping,* 33**,** 1076-1088.

LINDQUIST, M. A., GEUTER, S., WAGER, T. D. & CAFFO, B. S. 2019. Modular preprocessing pipelines can reintroduce artifacts into fMRI data. *Human Brain Mapping,* 40**,** 2358-2376.

LURIE, D. J., KESSLER, D., BASSETT, D. S., BETZEL, R. F., BREAKSPEAR, M., KHEILHOLZ, S., KUCYI, A., LIÉGEOIS, R., LINDQUIST, M. A., MCINTOSH, A. R., POLDRACK, R. A., SHINE, J. M., THOMPSON,

W. H., BIELCZYK, N. Z., DOUW, L., KRAFT, D., MILLER, R. L., MUTHURAMAN, M., PASQUINI, L., RAZI, A., VIDAURRE, D., XIE, H. & CALHOUN, V. D. 2020. Questions and controversies in the study of time-varying functional connectivity in resting fMRI. *Network Neuroscience,* 4**,** 30-69.

MA, X., ZHUO, Z., WEI, L., MA, Z., LI, Z. & LI, H. 2020. Altered Temporal Organization of Brief Spontaneous Brain Activities in Patients with Alzheimer's Disease. *Neuroscience,* 425**,** 1-11.

MUSCHELLI, J., NEBEL, M. B., CAFFO, B. S., BARBER, A. D., PEKAR, J. J. & MOSTOFSKY, S. H. 2014. Reduction of motion-related artifacts in resting state fMRI using aCompCor. *NeuroImage,* 96**,** 22-35.

NASREDDINE, Z. S., PHILLIPS, N. A., BÉDIRIAN, V., CHARBONNEAU, S., WHITEHEAD, V., COLLIN, I., CUMMINGS, J. L. & CHERTKOW, H. 2005. The Montreal Cognitive Assessment, MoCA: A Brief Screening Tool For Mild Cognitive Impairment. *Journal of the American Geriatrics Society,* 53**,** 695-699.

NEWMAN, M. E. J. & GIRVAN, M. 2004. Finding and evaluating community structure in networks. *Physical Review E,* 69**,** 026113.

ONODA, K. & YAMAGUCHI, S. 2013. Small-worldness and modularity of the resting-state functional brain network decrease with aging. *Neuroscience Letters,* 556**,** 104-108.

PARKES, L., FULCHER, B., YÜCEL, M. & FORNITO, A. 2018. An evaluation of the efficacy, reliability, and sensitivity of motion correction strategies for resting-state functional MRI. *NeuroImage,* 171**,** 415-436.

PEREIRA, J. B., MIJALKOV, M., KAKAEI, E., MECOCCI, P., VELLAS, B., TSOLAKI, M., KŁOSZEWSKA, I., SOININEN, H., SPENGER, C., LOVESTONE, S., SIMMONS, A., WAHLUND, L.-O., VOLPE, G., WESTMAN, E. & ADDNEUROMED CONSORTIUM, F. T. A. S. D. N. I. 2016. Disrupted Network Topology in Patients with Stable and Progressive Mild Cognitive Impairment and Alzheimer's Disease. *Cerebral Cortex,* 26**,** 3476-3493.

PINI, L., GEROLDI, C., GALLUZZI, S., BARUZZI, R., BERTOCCHI, M., CHITÒ, E., ORINI, S., ROMANO, M., COTELLI, M., ROSINI, S., MAGNALDI, S., MORASSI, M., COBELLI, M., BONVICINI, C., ARCHETTI, S., ZANETTI, O., FRISONI, G. B. & PIEVANI, M. 2020. Age at onset reveals different functional connectivity abnormalities in prodromal Alzheimer's disease. *Brain Imaging and Behavior*.

POSSIN, K. L., LALUZ, V. R., ALCANTAR, O. Z., MILLER, B. L. & KRAMER, J. H. 2011. Distinct neuroanatomical substrates and cognitive mechanisms of figure copy performance in Alzheimer's disease and behavioral variant frontotemporal dementia. *Neuropsychologia,* 49**,** 43-48.

POWER, JONATHAN D., COHEN, ALEXANDER L., NELSON, STEVEN M., WIG, GAGAN S., BARNES, KELLY A., CHURCH, JESSICA A., VOGEL, ALECIA C., LAUMANN, TIMOTHY O., MIEZIN, FRAN M., SCHLAGGAR, BRADLEY L. & PETERSEN, STEVEN E. 2011. Functional Network Organization of the Human Brain. *Neuron,* 72**,** 665-678.

PRUIM, R. H. R., MENNES, M., VAN ROOIJ, D., LLERA, A., BUITELAAR, J. K. & BECKMANN, C. F. 2015. ICA-AROMA: A robust ICA-based strategy for removing motion artifacts from fMRI data. *NeuroImage,* 112**,** 267-277.

QUEVENCO, F. C., PRETI, M. G., VAN BERGEN, J. M. G., HUA, J., WYSS, M., LI, X., SCHREINER, S. J., STEININGER, S. C., MEYER, R., MEIER, I. B., BRICKMAN, A. M., LEH, S. E., GIETL, A. F., BUCK, A., NITSCH, R. M., PRUESSMANN, K. P., VAN ZIJL, P. C. M., HOCK, C., VAN DE VILLE, D. & UNSCHULD, P. G. 2017. Memory performance-related dynamic brain connectivity indicates pathological burden and genetic risk for Alzheimer's disease. *Alzheimer's Research & Therapy,* 9**,** 24.

RUBINOV, M. & SPORNS, O. 2010. Complex network measures of brain connectivity: Uses and interpretations. *NeuroImage,* 52**,** 1059-1069.

SATTERTHWAITE, T. D., ELLIOTT, M. A., GERRATY, R. T., RUPAREL, K., LOUGHEAD, J., CALKINS, M. E., EICKHOFF, S. B., HAKONARSON, H., GUR, R. C., GUR, R. E. & WOLF, D. H. 2013. An improved

framework for confound regression and filtering for control of motion artifact in the preprocessing of resting-state functional connectivity data. *NeuroImage,* 64**,** 240-256.

SCHAEFER, A., KONG, R., GORDON, E. M., LAUMANN, T. O., ZUO, X.-N., HOLMES, A. J., EICKHOFF, S. B. & YEO, B. T. T. 2018. Local-Global Parcellation of the Human Cerebral Cortex from Intrinsic Functional Connectivity MRI. *Cerebral Cortex,* 28**,** 3095-3114.

SCHUMACHER, J., PERAZA, L. R., FIRBANK, M., THOMAS, A. J., KAISER, M., GALLAGHER, P., O'BRIEN, J. T., BLAMIRE, A. M. & TAYLOR, J.-P. 2019. Dynamic functional connectivity changes in dementia with Lewy bodies and Alzheimer's disease. *NeuroImage: Clinical,* 22**,** 101812.

SHAKIL, S., LEE, C.-H. & KEILHOLZ, S. D. 2016. Evaluation of sliding window correlation performance for characterizing dynamic functional connectivity and brain states. *NeuroImage,* 133**,** 111-128.

SHIRER, W. R., RYALI, S., RYKHLEVSKAIA, E., MENON, V. & GREICIUS, M. D. 2011. Decoding Subject-Driven Cognitive States with Whole-Brain Connectivity Patterns. *Cerebral Cortex,* 22**,** 158-165.

SPORNS, O. & BETZEL, R. F. 2016. Modular Brain Networks. *Annual Review of Psychology,* 67**,** 613-640.

STAM, C. J. 2014. Modern network science of neurological disorders. *Nature Reviews Neuroscience,* 15**,** 683-695.

TIAN, L., LI, Q., WANG, C. & YU, J. 2018. Changes in dynamic functional connections with aging. *NeuroImage,* 172**,** 31-39.

TIJMS, B. M., WINK, A. M., DE HAAN, W., VAN DER FLIER, W. M., STAM, C. J., SCHELTENS, P. & BARKHOF, F. 2013. Alzheimer's disease: connecting findings from graph theoretical studies of brain networks. *Neurobiology of Aging,* 34**,** 2023-2036.

VEITCH, D. P., WEINER, M. W., AISEN, P. S., BECKETT, L. A., CAIRNS, N. J., GREEN, R. C., HARVEY, D., JACK JR, C. R., JAGUST, W., MORRIS, J. C., PETERSEN, R. C., SAYKIN, A. J., SHAW, L. M., TOGA, A. W., TROJANOWSKI, J. Q. & ALZHEIMER'S DISEASE NEUROIMAGING, I. 2019. Understanding disease progression and improving Alzheimer's disease clinical trials: Recent highlights from the Alzheimer's Disease Neuroimaging Initiative. *Alzheimer's & Dementia,* 15**,** 106-152.

WANG, J., WANG, X., HE, Y., YU, X., WANG, H. & HE, Y. 2015. Apolipoprotein E ε4 modulates functional brain connectome in Alzheimer's disease. *Human Brain Mapping,* 36**,** 1828-1846.

WEINTRAUB, S., BESSER, L., DODGE, H. H., TEYLAN, M., FERRIS, S., GOLDSTEIN, F. C., GIORDANI, B., KRAMER, J., LOEWENSTEIN, D., MARSON, D., MUNGAS, D., SALMON, D., WELSH-BOHMER, K., ZHOU, X.-H., SHIRK, S. D., ATRI, A., KUKULL, W. A., PHELPS, C. & MORRIS, J. C. 2018. Version 3 of the Alzheimer Disease Centers' Neuropsychological Test Battery in the Uniform Data Set (UDS). *Alzheimer Disease & Associated Disorders,* 32.

YAMASHITA, K.-I., UEHARA, T., PRAWIROHARJO, P., YAMASHITA, K., TOGAO, O., HIWATASHI, A., TANIWAKI, Y., UTSUNOMIYA, H., MATSUSHITA, T., YAMASAKI, R. & KIRA, J.-I. 2019. Functional connectivity change between posterior cingulate cortex and ventral attention network relates to the impairment of orientation for time in Alzheimer's disease patients. *Brain Imaging and Behavior,* 13**,** 154-161.

YEO, B. T., KRIENEN, F. M., SEPULCRE, J., SABUNCU, M. R., LASHKARI, D., HOLLINSHEAD, M., ROFFMAN, J. L., SMOLLER, J. W., ZÖLLEI, L., POLIMENI, J. R., FISCHL, B., LIU, H. & BUCKNER, R. L. 2011. The organization of the human cerebral cortex estimated by intrinsic functional connectivity. *Journal of Neurophysiology,* 106**,** 1125-1165.

ZALESKY, A., FORNITO, A., COCCHI, L., GOLLO, L. L. & BREAKSPEAR, M. 2014. Time-resolved resting-state brain networks. *Proceedings of the National Academy of Sciences,* 111**,** 10341.